

# Dystrophin protects the sarcolemma from stresses developed during muscle contraction

(muscular dystrophy/muscle injury/*mdx* mouse)

BASIL J. PETROF\*, JOSEPH B. SHRAGER<sup>†</sup>, HANSELL H. STEDMAN<sup>†</sup>, ALAN M. KELLY<sup>‡</sup>,  
AND H. LEE SWEENEY<sup>§¶</sup>

\*Pulmonary and Critical Care Division and Center for Sleep and Respiratory Neurobiology, and Departments of <sup>†</sup>Surgery and <sup>§</sup>Physiology, University of Pennsylvania School of Medicine, and <sup>‡</sup>Department of Pathobiology, University of Pennsylvania School of Veterinary Medicine, Philadelphia, PA 19104

Communicated by C. Richard Taylor, January 19, 1993

**ABSTRACT** The protein dystrophin, normally found on the cytoplasmic surface of skeletal muscle cell membranes, is absent in patients with Duchenne muscular dystrophy as well as *mdx* (X-linked muscular dystrophy) mice. Although its primary structure has been determined, the precise functional role of dystrophin remains the subject of speculation. In the present study, we demonstrate that dystrophin-deficient muscle fibers of the *mdx* mouse exhibit an increased susceptibility to contraction-induced sarcolemmal rupture. The level of sarcolemmal damage is directly correlated with the magnitude of mechanical stress placed upon the membrane during contraction rather than the number of activations of the muscle. These findings strongly support the proposition that the primary function of dystrophin is to provide mechanical reinforcement to the sarcolemma and thereby protect it from the membrane stresses developed during muscle contraction. Furthermore, the methodology used in this study should prove useful in assessing the efficacy of dystrophin gene therapy in the *mdx* mouse.

Duchenne muscular dystrophy (DMD) is the most common of the human muscular dystrophies. The cause of the disease is a lack of the protein dystrophin, which is normally found on the cytoplasmic surface of skeletal muscle cell membranes (1, 2). Dystrophin is also absent in *mdx* (X-linked muscular dystrophy) mice (3). Intriguingly, in the case of the *mdx* mouse, only the diaphragm displays the muscle pathology typical of human DMD patients (4). Although elements of the dystrophin gene and protein structure have been determined (5, 6), the functional role of dystrophin has not been ascertained. Leading candidates for the basic functional defect in dystrophin-deficient muscle include (i) primary structural weakness of the sarcolemma (7, 8) and (ii) a specific increase in membrane permeability to Ca<sup>2+</sup> because of altered ion channel function (9, 10). In support of the former, it has been reported that isolated adult muscle fibers as well as cultured muscle cells from *mdx* mice demonstrate increased susceptibility to rupture from hypoosmotic shock (7). However, the relevance of this model to *in vivo* muscle function has recently been called into question (11). Other investigators have found no difference in the suction pressure required to rupture the sarcolemma of normal and *mdx* myotubes (10). The presence of altered Ca<sup>2+</sup> ion regulation in dystrophic muscle is supported by reports that the open probability of Ca<sup>2+</sup> channels is increased in dystrophin-deficient muscle (9, 10). Previous work in other experimental models suggests that such Ca<sup>2+</sup> leakage could play a role in producing sarcolemmal damage (12, 13).

We have postulated (4) that the predilection of the *mdx* mouse diaphragm to undergo degeneration (in contrast to the limb muscles) reflects the relatively greater work rate performed by the diaphragm vs. other muscles in this species. If the primary function of dystrophin is to provide structural integrity to the muscle membrane, one would predict that the major determinant of membrane damage would be the level of membrane stress associated with contraction rather than the number of muscle activations. If, on the other hand, the fundamental problem in dystrophin-deficient muscle is an inability to handle Ca<sup>2+</sup>, then the high Ca<sup>2+</sup> load associated with repeated muscle activation (14) should result in the greatest level of damage. The present study was designed to ascertain the relative importance of these two potential mechanisms of contraction-induced injury in dystrophin-deficient muscle.

## MATERIALS AND METHODS

**Muscle Preparations.** Either costal diaphragm strips or intact extensor digitorum longus (EDL) muscles were dissected from 90- to 110-day-old control (C57BL/10ScSn) and *mdx* mice. Muscles were immersed in physiologic solution containing a low molecular weight dye (0.2% procion orange in Ringer's solution) buffered to pH 7.4 with 25 mM HEPES, which was continuously oxygenated and maintained at 23 ± 0.5°C. Muscles were mounted horizontally in a muscle bath, attached by their bony or tendinous insertions to a platform at one end and to the lever of a dual-mode servomotor system (allowing force measurements as well as changes in muscle length by a predetermined velocity and amount) at the other. Stimulation was induced by using two platinum plate electrodes placed on both sides of the muscle, which was then adjusted to that length (*L*<sub>0</sub>) that allowed maximal twitch force to be achieved. Once *L*<sub>0</sub> was thus identified, muscle fiber length was measured with fine calipers.

**Experimental Protocols.** Control and *mdx* muscles were subjected to one of the following protocols: (i) ECC, an eccentric contraction regimen, consisting of five maximal (fused tetani) stimulation periods (frequency of 80 Hz for 700-ms duration), with the muscle being lengthened at a velocity of 0.5 *L*<sub>0</sub>/s through a distance of 10% *L*<sub>0</sub> during the final 200 ms; (ii) ISO, an isometric regimen, also consisting of 5 maximal (fused tetani) stimulation periods, with muscle length maintained at *L*<sub>0</sub> and the force-time integral matched to the eccentric protocol; and (iii) PAS, passive lengthenings without muscle stimulation, with the lengthening parameters matched to the eccentric protocol. In protocols *i-iii*, a 4-min

Abbreviations: DMD, Duchenne muscular dystrophy; EDL, extensor digitorum longus.

<sup>¶</sup>To whom reprint requests should be addressed at: Department of Physiology, University of Pennsylvania School of Medicine, 37th Street and Hamilton Walk, Philadelphia, PA 19104-6085.

The publication costs of this article were defrayed in part by page charge payment. This article must therefore be hereby marked "advertisement" in accordance with 18 U.S.C. §1734 solely to indicate this fact.

recovery period was allowed between each of the stimulations or passive lengthenings, with muscle length being maintained at  $L_o$ . A fourth protocol, ISO rep, consisted of repeated submaximal (unfused tetani) isometric stimulation (frequency of 30 Hz, 0.33 duty cycle, 90 trains per min) over a 5-min period ( $\approx 450$  contractions) at  $L_o$ . Regardless of the experimental protocol employed, the stimulated muscle and its non-stimulated contralateral counterpart (serving as an internal control) were both submerged in the oxygenated 0.2% procion orange/Ringer's solution for a total duration of 90 min. The muscles were then rinsed in normal Ringer's solution for 5 min twice, after which they were rapidly frozen in isopentane precooled with liquid  $N_2$  and stored at  $-70^\circ C$  for later analysis.

**Assessment of Sarcolemmal Damage.** Muscles were sectioned at mid-belly, and the percentage of dye-positive fibers on each muscle section (mean number [ $\pm$ SEM] of fibers counted: diaphragm,  $1109 \pm 46$ ; EDL,  $567 \pm 37$ ) were determined by two observers blinded to the identity of the samples and were averaged. (The fiber counts of the two observers were within 10% of each other for all muscles included in this study.) Edges of the sections (within 1.0 mm of the plane of dissection) were excluded to avoid fibers potentially damaged as a result of muscle dissection. The fiber cross-sectional area was determined from high-magnification photographs by using a computer-based image-processing system. To assess differences between groups (control vs. *mdx*), Student's two-tailed *t* test for independent samples was applied. Differences between muscles (dia-

phragm vs. EDL) within each group were determined by using Student's two-tailed *t* test for dependent samples. A first-order regression model was used to examine the relationship between peak force generation and the percentage of dye-positive fibers. To assess potential differences in regression line slopes between *mdx* and control muscles, a cross-product interaction term was introduced and a two-tailed *t* test was performed. Statistical significance was defined as  $P < 0.05$ .

## RESULTS AND DISCUSSION

Sarcolemmal disruptions were detected in transversely sectioned muscle by using a fluorescent, low-molecular weight dye (procion orange,  $M_r$  631) to which intact muscle cells are impermeable (15, 16). Rapid passage of the dye through disrupted cellular membranes allows detection of damaged fibers (Fig. 1). While it is known that repeated eccentric contractions, which generate high peak stress, lead to extensive injury in both normal and dystrophic muscle (17–19), we examined a range of contraction conditions to expose differential responses. Control and *mdx* muscles were subjected to one of the following protocols: (i) high peak stress (eccentric contraction; ECC protocol) with few activations (see Fig. 2); (ii) moderate peak stress (isometric contraction; ISO protocol) with few activations; (iii) low peak stress without activation (passive stretch; PAS protocol); and (iv) low peak stress with a large number of activations (submaximal isometric contraction; ISO rep protocol). A hindlimb muscle

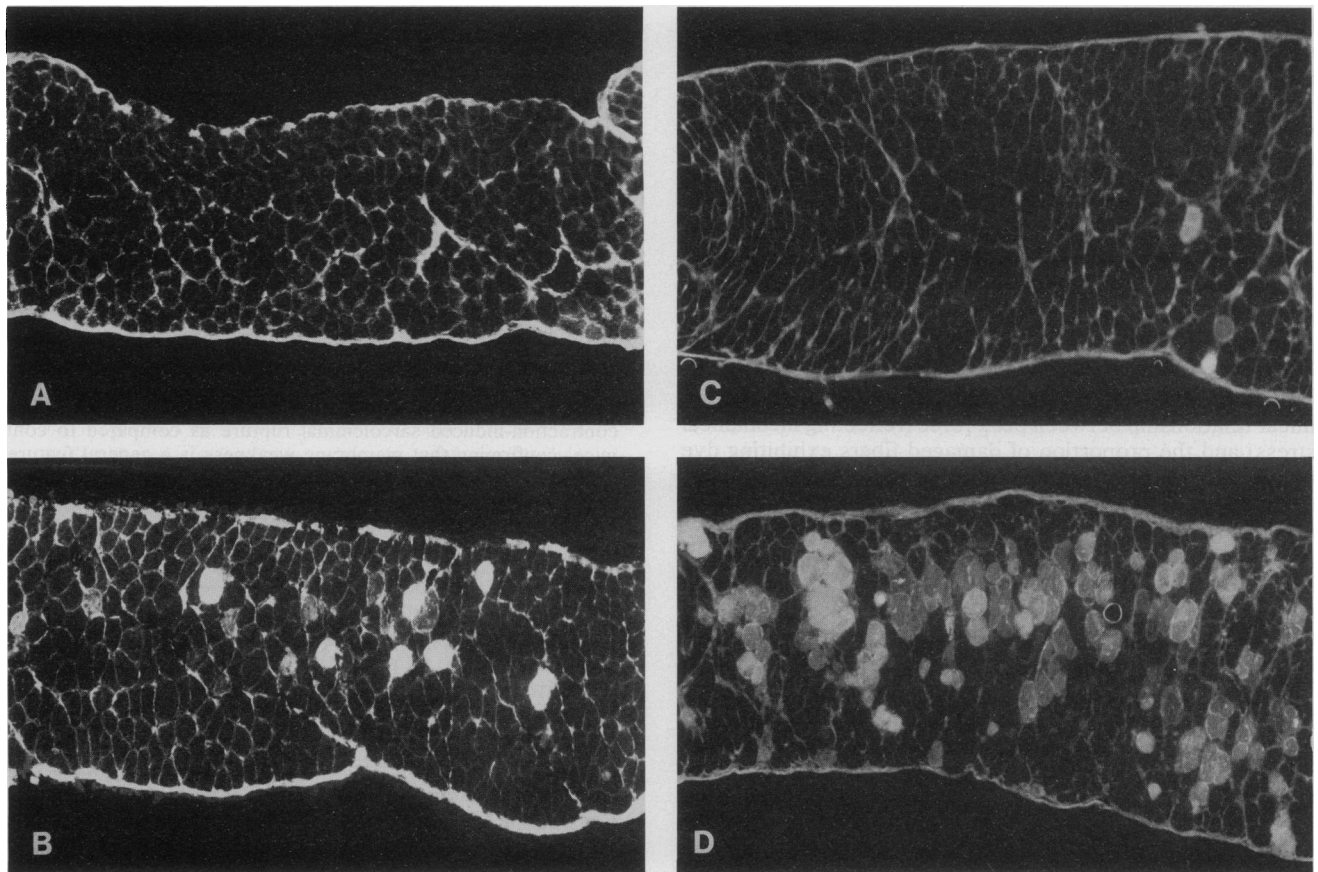


FIG. 1. Transverse frozen sections of diaphragm muscles from *mdx* and control C57B/10 mice, after immersion in procion orange dye, examined under fluorescence microscopy. (A) Control diaphragm, not subjected to *in vitro* contraction protocols. Although there is dye penetration into the muscle (as shown by intense staining of connective tissue throughout the section), there is an absence of dye uptake within individual muscle fibers. (B) Control diaphragm after eccentric contraction (ECC protocol). Note the presence of a few fibers into which the dye has penetrated, indicating sarcolemmal disruption. (C) *mdx* diaphragm, not subjected to contraction protocol. (D) *mdx* diaphragm after eccentric contraction (ECC protocol). Note the large increase in the proportion of fibers containing dye. ( $\times 100$ .)

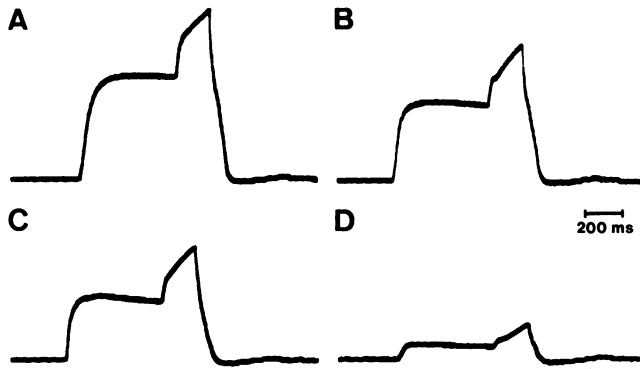


FIG. 2. Oscilloscopic tracings of force vs. time during maximal diaphragm stimulation with isometric contraction over the initial 500 ms and eccentric component during the last 200 ms (ECC protocol). Traces: A and B, control diaphragm, initial contraction (trace A) and final (fifth) contraction (trace B); C and D, *mdx* diaphragm, initial contraction (trace C) and final contraction (trace D). Note the large increase in peak force achieved during the eccentric component of the contraction. A decrease in isometric force (which excludes tension produced by stretch *per se* and thus reflects muscle fiber force-generating capacity alone) occurred in both control and *mdx* muscles at the completion of the five maximal contractions, consistent with the presence of fiber damage. This decrease (as a percentage of initial force) was substantially greater in the *mdx* muscle, indicating a higher level of global muscle injury. For the entire group of *mdx* and control muscles subjected to the ECC protocol, mean values ( $\pm$ SEM) for final force amounted to  $43.1 \pm 5.7\%$  and  $71.3 \pm 10.2\%$  of initial force, respectively ( $P < 0.05$ ).

(EDL) was also subjected to the ECC protocol to ascertain whether the diaphragm response is representative of the *mdx* musculature.

Dystrophin-deficient and normal muscle fibers suffered sarcolemmal breakage during muscle contraction. However, the magnitude of damage was greater in *mdx* diaphragm and EDL muscles in all cases (Fig. 3). Eccentric contractions (ECC protocol), during which the highest peak force and membrane stress are generated, resulted in the greatest dye uptake. Maximal isometric activation (ISO protocol) of the diaphragm and repeated submaximal isometric activations (ISO rep protocol) caused less dye uptake than the ECC protocol, whereas passive stretch (PAS protocol) caused an increase in dye uptake in *mdx* muscle only.

In both *mdx* and control muscle, there was a significant linear relationship between peak force (reflecting mechanical stress) and the proportion of damaged fibers exhibiting dye uptake (Fig. 4). For any given level of peak force, however, there was a higher percentage of damaged fibers in *mdx* muscle. Additionally, the slope of the relationship between peak force generation and dye-positive fibers was increased in *mdx* vs. control muscles ( $P < 0.05$ ). There was no relationship between the number of muscle activations and the proportion of damaged fibers in either *mdx* ( $r = 0.05$ ) or control ( $r = 0.11$ ) muscles. Note in Fig. 3 that despite a 10-fold increase in the number of activations in the ISO rep protocol vs. the ISO protocol, there was no significant difference in the proportion of damaged *mdx* muscle fibers. Moreover, passive stretch of *mdx* muscle in the absence of activation also resulted in damaged fibers.

Muscle contraction generates longitudinal forces (parallel to the myofilaments), which are transmitted to bone via tendon. Radial forces are also developed by crossbridges during muscle contraction (20, 21). Consistent with this, it has been demonstrated that compression of the myofilament lattice occurs during muscle contraction, with the degree of compression being greater during eccentric rather than isometric contractions (20). Since the myofilaments are ultimately anchored in the surface membrane (21, 22), such

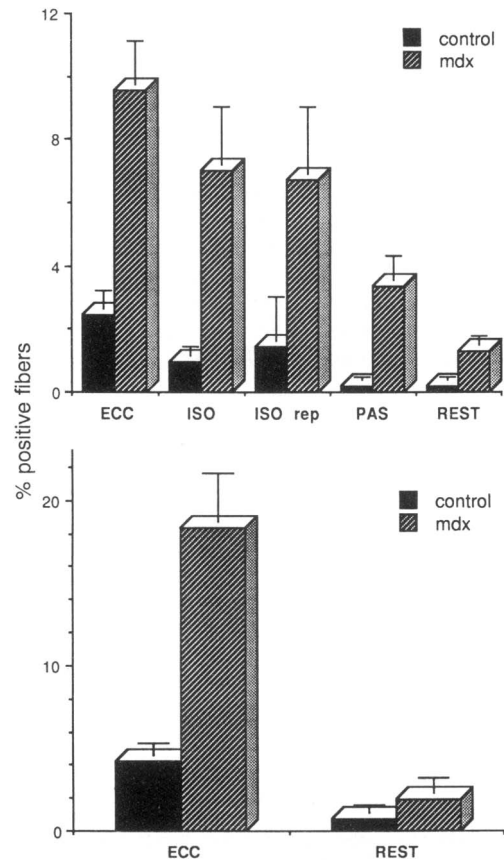


FIG. 3. Percentage of positive (i.e., dye-containing) fibers in control (solid bars) and *mdx* (hatched bars) mouse skeletal muscle sections. Values are means  $\pm$  SEM (for each muscle and protocol,  $n = 5$  or 6). (Upper) Diaphragm. Bars: ECC protocol, after five maximal contractions with eccentric component; ISO protocol, after five maximal isometric contractions; ISO rep protocol, after 450 submaximal isometric contractions; PAS protocol, after five passive lengthenings; REST, after no stimulation or mechanical manipulation. (Lower) EDL. Bars: ECC protocol, after five maximal contractions with eccentric component; REST, after no stimulation or mechanical manipulation. The REST group consisted of the contralateral muscles from the same animals simultaneously immersed in dye for an identical period but without the above physiologic manipulations. Muscle fibers of both the *mdx* diaphragm ( $P < 0.01$ ) and EDL ( $P < 0.001$ ) demonstrated an increased susceptibility to contraction-induced sarcolemmal rupture as compared to control mice, confirming that membrane weakness is a general feature of dystrophin-deficient muscle.

radial forces are necessarily transmitted to the sarcolemma and thereby exert tension upon the membrane. Muscle fiber membranes have presumably evolved structural elements that render them capable of withstanding both longitudinally and radially directed mechanical stresses. The cytoskeletal protein spectrin is proposed to play such a role in the membrane of erythrocytes (23). Dystrophin, which exhibits significant homology to spectrin (24), would appear to serve this function in muscle fiber membranes.

One can envision at least two mechanisms whereby dystrophin could help to stabilize the sarcolemma during muscle contraction. First, dystrophin could help to distribute the mechanical forces associated with contraction over a broader membrane area by interacting with other structural elements exerting tension upon the sarcolemma. Second, the recent finding of a dystrophin-associated glycoprotein complex spanning the sarcolemma raises the possibility that forces could be transmitted across and beyond the membrane to the extracellular matrix (25, 26). It has recently been shown (27) that severe childhood autosomal recessive muscular dystro-

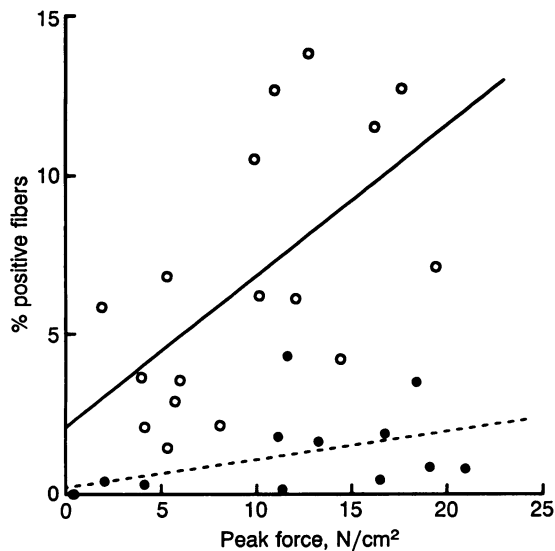


FIG. 4. Relationship between peak force (corrected for muscle cross-sectional area) and percentage of positive (dye-containing) fibers in control (●) and *mdx* (○) diaphragm muscle sections pooled from the ECC, ISO and PAS protocol groups displayed in Fig. 3. Regression analysis revealed a significant correlation between the two variables for both control (dashed line,  $y = 0.09x + 0.21$ ;  $r = 0.52$ ;  $P < 0.05$ ) and *mdx* (solid line,  $y = 0.47x + 2.1$ ;  $r = 0.60$ ;  $P < 0.01$ ) muscles. The slopes of the relationship differed ( $P < 0.05$ ) between control and *mdx* fibers, such that any given increment in peak force resulted in a greater increase in the percentage of positive fibers in the *mdx* group.

phy (SCARMD), a disease with a DMD-like phenotype, results from a deficiency of one component of the dystrophin-associated glycoprotein complex (the 50-kDa subunit). While the phenotype of this disease is generally less severe than DMD (28), this observation suggests that full protection against contraction-generated stresses may require association of the dystrophin-cytoskeletal network with the dystrophin-associated glycoprotein complex, which ultimately provides mechanical linkage to the extracellular matrix.

Increases in fiber size result in a decreased surface-to-volume ratio, leading to a higher level of membrane stress during force development. Accordingly, the EDL [mean fiber size,  $1058 \pm 615 \mu\text{m}^2$  (SEM)] exhibited a greater degree of dye uptake than the diaphragm [mean fiber size,  $735 \pm 28 \mu\text{m}^2$  (SEM)] during the ECC protocol ( $P < 0.05$ ). This finding is also consistent with a previous report that larger, type IIb fibers are most severely affected in the limb muscles of children with DMD (29). Furthermore, this may help to explain the fact that limb muscles of humans are affected to a far greater extent by the absence of dystrophin than are those of mice, since humans have an average fiber cross-sectional area that is 2–3 times that of mouse fibers (30). Presumably, the disproportionately large work rate performed by the mouse diaphragm overcomes the relative protection afforded by smaller fiber size (31), thereby leading to degeneration (4).

These findings have important implications for the treatment of DMD. Whether dystrophin deficiency alters the susceptibility of muscle to exercise-induced injury has been the subject of contention (11, 17–19). Patients with DMD have been encouraged to participate in exercise programs (32), and breathing against high levels of airway resistance has been advocated as a means of strengthening the diaphragm (33). Our results suggest that high-force muscular contractions contribute to the progression of DMD by accelerating the rate of fiber damage and therefore should be avoided. Furthermore, the methodology used in this study

may provide an assay for assessing the functional consequences of dystrophin replacement in *mdx* muscle.

Injury and repair are likely the normal route of adaptation to increased utilization and stress production in skeletal muscle (34–36). However, the present study demonstrates that the extent of damage is significantly higher in dystrophic muscle for any given level of stress. Thus, dystrophin deficiency shifts the normal balance between injury and repair towards the former by lowering the threshold for contraction-induced damage. Ultimate degeneration of dystrophin-deficient muscle would therefore appear to result from the cumulative effects of heightened membrane fragility, with eventual overloading of muscle regenerative capacity.

We thank Dr. Michael Reedy for suggesting the use of procion orange in these experiments. This work was supported by grants from the Muscular Dystrophy Association, the National Institutes of Health (AR35661 and HL15835), and the Medical Research Council of Canada. H.L.S. is an Established Investigator of the American Heart Association.

1. Watkins, S. C., Hoffman, E. P., Slayter, H. S. & Kunkel, L. M. (1988) *Nature (London)* **333**, 863–866.
2. Hoffman, E. P., Brown, R. H. & Kunkel, L. M. (1987) *Cell* **51**, 919–928.
3. Sicinski, P., Geng, Y., Ryder-Cook, A. S., Barnard, E. A., Darlison, M. G. & Barnard, P. J. (1989) *Science* **244**, 1578–1580.
4. Stedman, H. H., Sweeney, H. L., Shrager, J. B., Maguire, H. C., Panettieri, R. A., Petrof, B. J., Narusawa, M., Leferovich, J., Sladky, J. T. & Kelly, A. M. (1991) *Nature (London)* **352**, 536–539.
5. Koenig, M., Hoffman, E. P., Bertelson, C. J., Monaco, A. P., Feener, C. & Kunkel, L. M. (1987) *Cell* **50**, 509–517.
6. Koenig, M., Monaco, A. P. & Kunkel, L. M. (1988) *Cell* **53**, 219–228.
7. Menke, A. & Jockusch, H. (1991) *Nature (London)* **349**, 69–71.
8. Karpati, G. & Carpenter, S. (1986) *Am. J. Med. Genet.* **25**, 653–658.
9. Fong, P., Turner, P. R., Denetclaw, W. F. & Steinhardt, R. A. (1990) *Science* **250**, 673–676.
10. Franco, A. & Lansman, J. B. (1990) *Nature (London)* **344**, 670–673.
11. Jackson, M. J., McArdle, A., Edwards, R. H. & Jones, D. A. (1991) *Nature (London)* **350**, 664.
12. Jones, D. A., Jackson, M. J., McPhail, G. & Edwards, R. H. T. (1984) *Clin. Sci.* **66**, 317–322.
13. Duncan, C. J. & Jackson, M. J. (1987) *J. Cell Sci.* **87**, 183–188.
14. Turner, P. R., Westwood, T. M., Regen, C. M. & Steinhardt, R. A. (1988) *Nature (London)* **335**, 735–738.
15. Bradley, W. G. & Fulthorpe, J. J. (1978) *Neurology* **28**, 670–677.
16. Stead, C. V. (1973) in *Intracellular Staining in Neurobiology*, eds. Kater, S. B. & Nicholson, C. (Springer, Berlin), pp. 41–59.
17. Weller, B., Karpati, G. & Carpenter, S. (1990) *J. Neurol. Sci.* **100**, 9–13.
18. McArdle, A., Edwards, R. H. T. & Jackson, M. J. (1991) *Clin. Sci.* **80**, 367–371.
19. Sacco, P., Jones, D. A., Dick, J. R. T. & Vrbova, G. (1992) *Clin. Sci.* **82**, 227–236.
20. Cecchi, G., Bagni, M. A., Griffiths, P. J., Ashley, C. C. & Maeda, Y. (1990) *Science* **250**, 1409–1411.
21. Street, S. F. (1983) *J. Cell. Physiol.* **114**, 346–364.
22. Pierobon-Bormioli, S. (1981) *J. Muscle Res. Cell Motil.* **2**, 401–413.
23. Waugh, R. E. & Agre, P. J. (1988) *J. Clin. Invest.* **81**, 133–141.
24. Davison, M. D. & Critchley, D. R. (1988) *Cell* **52**, 159–160.
25. Ervasti, J. M. & Campbell, K. P. (1991) *Cell* **66**, 1121–1131.
26. Ibraghimov-Beskrovnyaya, O., Ervasti, J. M., Leveille, C. J., Slaughter, C. A., Sernett, S. W. & Campbell, K. P. (1992) *Nature (London)* **355**, 696–702.
27. Matsumura, K., Tome, F. M. S., Collin, H., Azibi, K., Chaouch, M., Kaplan, J.-C., Fardeau, M. & Campbell, K. P. (1992) *Nature (London)* **359**, 320–322.
28. Ben Hamida, M., Fardeau, M. & Attia, N. (1983) *Muscle Nerve* **6**, 469–480.

29. Webster, C., Silberstein, L., Hays, A. P. & Blau, H. M. (1988) *Cell* **52**, 503–513.
30. Mizuno, M. & Secher, N. H. (1989) *J. Appl. Physiol.* **67**, 592–598.
31. Karpati, G., Carpenter, S. & Prescott, S. (1988) *Muscle Nerve* **11**, 795–803.
32. Walton, J. (1988) in *Disorders of Voluntary Muscle*, ed. Walton, J. (Churchill Livingstone, New York), pp. 561–613.
33. DiMarco, A. F., Kelling, J. S., DiMarco, M. S., Jacobs, I., Shields, R. & Altose, M. D. (1985) *Muscle Nerve* **8**, 284–290.
34. McCully, K. K. & Faulkner, J. A. (1985) *J. Appl. Physiol.* **59**, 119–126.
35. Jones, D. A., Newham, D. J., Round, J. M. & Tolfree, S. E. J. (1986) *J. Physiol. (London)* **375**, 435–448.
36. Kasper, C. E., White, T. P. & Maxwell, L. C. (1990) *J. Appl. Physiol.* **68**, 533–539.